

Article

A Statistical–Distributed Model of Average Annual Runoff for Water Resources Assessment in DPR Korea

Tongho Ri ¹, Jiping Jiang ^{2,3,*} , Bellie Sivakumar ^{4,5}  and Tianrui Pang ^{3,6}

¹ Department of Global Environmental Science, Kim Il Sung University, Pyongyang 999093, Korea; jjp_lab@sina.com

² State Key Laboratory of Urban Water Resource and Environment, Harbin Institute of Technology, Harbin 150090, China

³ Shenzhen Municipal Engineering Lab of Environmental IoT Technologies, School of Environmental Science and Engineering, Southern University of Science and Technology, Shenzhen 518055, China; nicolaser941225@gmail.com

⁴ School of Civil and Environmental Engineering, University of New South Wales, Sydney, NSW 2052, Australia; s.bellie@unsw.edu.au

⁵ State Key Laboratory of Hydrosience and Engineering, Tsinghua University, Beijing 100084, China

⁶ School of Environment, Harbin Institute of Technology, Harbin 150090, China

* Correspondence: jiangjp@sustech.edu.cn

Received: 26 March 2019; Accepted: 6 May 2019; Published: 8 May 2019



Abstract: Water resource management is critical for the economic development of the Democratic People’s Republic of Korea (DPRK), where runoff plays a central role. However, long and continuous runoff data at required spatial and temporal scales are generally not available in many regions in DPRK, the same as in many countries around the world. A common practice to fill the gaps is to use some kind of interpolation or data-infilling methods. In this study, the gaps in annual runoff data were filled using a distributed runoff map. A novel statistical–distributed model of average annual runoff was derived from 50 years’ observation on 200 meteorological observation stations in DPRK, considering the influence of climatic factors. Using principal component analysis, correlation analysis and residual error analysis, average annual precipitation, average annual precipitation intensity, average annual air temperature, and hot seasonal air temperature were selected as major factors affecting average annual runoff formation. Based on the water balance equation and assumptions, the empirical relationship for runoff depth and impact factors was established and calibrated. The proposed empirical model was successfully verified by 93 gauged stations. The cartography of the average annual runoff map was automatically implemented in ArcGIS. A case study on the Tumen River Basin illustrated the applicability of the proposed model. This model has been widely used for the development and management of water resources by water-related institutes and design agencies in DPRK. The limitation of the proposed model and future works are also discussed, especially the impacts of climate changes and topology changes and the combination with the physical process of runoff formation.

Keywords: average annual runoff; runoff map; hydrological model; GIS; DPR Korea

1. Introduction

Research regarding water resources estimation at regional and continental level contributes a lot in establishing water resources management policy [1–3], and water resources assessment is the first step for water resources development. Runoff plays a central role in water resources assessment. Generally, water resources are evaluated by means of average annual runoff [4,5], the mathematical expectation of multiyear observations of annual runoff, and can be described as runoff depth [4,6–12].

Usually, in hydrologic modeling, a water balance equation is used for the computation of average annual runoff, keeping in mind the factors affecting annual runoff [5,9,13–19].

Usually, average annual runoff is computed by means of multiyear data, while in some cases, from one-year data. However, long and continuous runoff data at required spatial and temporal scales are generally not available in many regions around the world, due to the costs involved in measurements, difficulty in accessing the locations of interest, and malfunctioning of the measurement devices, among others. A common practice to fill the gaps is to use some kind of interpolation or data-infilling methods. Many average annual runoff models have been reported for water resources development in regions which lack observational data [1,4,8,12,20–22]. The accuracy of the average annual runoff model mainly depends on the factors affecting annual runoff [23–27], which can be computed by principal component analysis and the factor analysis method [11,28,29].

Research has confirmed that the factors affecting runoff formation vary with locality [17]. It is well accepted that precipitation is the main meteorological factor for runoff formation [22]. The physical characteristics of the watershed underlying surface also play an important role, which includes land use, soil type, slope, vegetation, etc. [30–32]. Human activities like agriculture irrigation, urban water supply, and drainage, water division projects inevitably lead to changes in water resources.

Recently, lots of hydrological progress has been observed in modeling spatial variation of precipitation, infiltration, and evaporation with the advancement in 3S technology (GIS—geographic information system, RS—remote sensing, and GPS—global position system) [33] and computer information processing [5,34–38]. It is highly practiced in those regions for runoff estimation which lacks observational data, i.e., ungauged areas, for evaluating water resources.

Runoff maps are frequently used for highlighting spatiotemporal changes in water resources [10,20,39–42], while maps of meteorology factors are used for interpreting spatiotemporal changes in precipitation [13], evaporation [5], catchment classification, estimation of hydrologic response in ungauged catchments [10,12], etc.

In general, average annual runoff is computed by methods based on the geometric center of the river basin. Such methods, however, often fail to provide reliable runoff maps for small- and medium-sized rivers. Since hydrologic models take into account the local natural geographic, climatic, hydrologic characteristics and local data, such models are very useful for generating runoff maps in small and medium-sized rivers.

This study was rooted in the Democratic People's Republic (DPR) of Korea, where very limited hydrology studies were reported in the literature. Scientific water resources management is critical for the recent economic reformation and opening up of DPR Korea. Runoff-based water resources assessment on the whole nation is significant. However, due to the data limitation, advanced hydrology models with high resolution are not applicable in DPR Korea. An empirical statistical approach to produced distributed runoff results is preferred, especially for ungauged areas. Therefore, we attempted to address these issues in the present study. Making good use of 50 years of records in 200 meteorological stations, a statistical–distributed average annual runoff model was developed in this work.

The rest of this paper is organized as follows: In Section 2, the climate condition and the water balance relationship in DPR Korea is described. The factors affecting the average annual runoff are analyzed by principal component analysis (PCA) and explained. In Section 3, the new statistical annual runoff model is clearly described. Furthermore, model verification and cartography of the runoff map in GIS are presented. Section 4 presents the analysis and results for the Tumen River Basin. Sections 5 and 6 discuss and conclude the research.

2. Rainfall–Runoff Relationship and Runoff Impact Factors

2.1. The Precipitation and Temperature Characteristics in DPR Korea

DPR Korea has a temperate monsoon climate, four distinct seasons, average annual temperature varies from 8 °C to 12 °C, and average annual precipitation varies from 1000 to 1200 mm. Most of the

precipitation falls in July–August (see Figures 1 and 2). Average annual monthly temperature and precipitation characteristics are shown in Table 1.

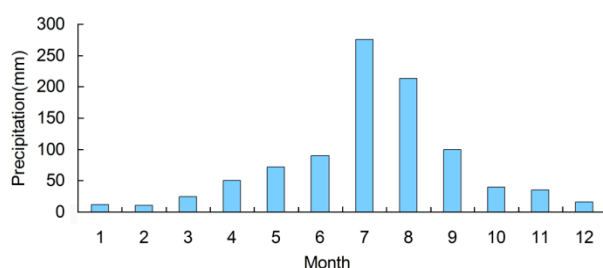


Figure 1. The monthly distribution of precipitation in the Democratic People’s Republic (DPR) of Korea.

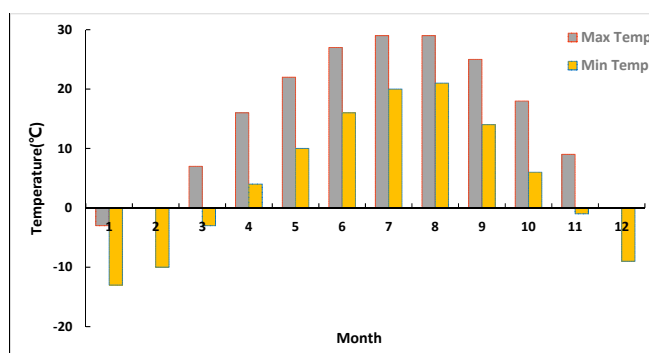


Figure 2. The monthly distribution of temperature in DPR Korea.

Table 1. The average annual temperature and precipitation in DPR Korea.

Month	Jan	Feb	Mar	Apr	May	Jun	Jul	Aug	Sep	Oct	Nov	Dec
Average daily maximum temperatures (°C)	-1	2	9	17	23	27	29	29	25	18	9	2
Average daily minimum temperature (°C)	-11	-8	-2	5	11	16	21	20	14	7	0	-7
Average precipitation amount (mm)	12	11	25	50	72	90	275	213	100	40	35	16
Average precipitation days (d)	5	4	5	7	8	9	14	11	7	6	7	6

2.2. Watershed Water Balance Relationship

Annual runoff is computed using the classical water balance Equation [43]:

$$Y = P - E \pm \Delta S \tag{1}$$

where Y is the annual runoff depth (mm); P is the annual amount of precipitation (mm); E is the annual amount of evaporation (mm); and ΔS is the change in water storage.

The change in basin water storage can be ignored, i.e., equal to zero, when considering multiyear average (see Equation (2)):

$$Y = P - E \tag{2}$$

Equation (2) can also be denoted by annual runoff coefficient $\varphi = Y/P$ and annual evaporation coefficient $\eta_E = E/P$.

$$\varphi = 1 - \eta \tag{3}$$

E can be computed indirectly by hydrometeorological observations using the values of P and Y . Calculating the values of E is challenging due to the influences from climatic factors, geographical factors, etc. [44]. Since soil type affects water exchanges with the atmosphere, Reder et al. evaluated the sensitivity of the annual average of runoff, precipitation, evaporation, and deep drainage to different soil types in China and argued the importance of clarifying the role of “geomorphological factors” [30]. Li et al. found that the effect of climate change on evapotranspiration was much more significant than the effect of land use and land cover changes in China [44].

Usually, the average annual runoff model is formulated by establishing a relationship between the parameters and elucidating the influence of factors affecting evaporation E or evaporation coefficient η_E .

In DPR Korea, the correlation coefficient between rainfall and runoff varies from 0.90 to 0.98, which makes the surface water consistent throughout the year. There are regional differences among river runoff, but 60% to 80% runoff flows occur in the summer.

2.3. Factors Affecting the Annual Runoff Formation by PCA

Time series of the main factors affecting runoff formation can be obtained using the principal component analysis method. The basic data matrix can be configured as follows:

$$Y(p \times n) = \begin{bmatrix} y_{11} & y_{12} & \cdots & y_{1n} \\ y_{21} & y_{22} & \cdots & y_{2n} \\ \vdots & \vdots & \cdots & \vdots \\ y_{p1} & y_{p2} & \cdots & y_{pn} \end{bmatrix}, \tag{4}$$

where y is annual runoff; p is the size of observational series; and n is the number of observation stations.

Then, the measured values can be represented as follows:

$$Y(t, x) = T_1(t)x_1(x) + T_2(t)x_2(x) + \cdots + T_m(t)x_m(x) \tag{5}$$

Or:

$$Y(t, x) = \sum_{k=1}^m T_k(t)X_k(x) \tag{6}$$

where $T_k(t)$ is the coefficient related to the time; $X_k(x)$ is the function characterizing the distribution field; and m is the number of factors affecting average annual runoff formation, $k = 1, 2, \dots, g, \dots, m$.

Standardizing basis data and evolving obtains an $n \times n$ correlation matrix. It should satisfy a relationship of $m \leq n$. In this case, the principal component analysis model can be obtained as follows:

$$(R - \lambda I)X = 0 \tag{7}$$

where R is correlation matrix and I is a unit matrix.

The characteristic equation is:

$$|R - \lambda I| = 0 \tag{8}$$

Time coefficient matrix is:

$$T_{gz} = \frac{\sum_{z=1}^m Y_{tz}X_{gz}}{\sum_{z=1}^m X_{gz}^2} \tag{9}$$

where $z = 1, 2, \dots, m$.

The contribution rate is:

$$\beta = \frac{\lambda_k}{\sum_{k=1}^m \lambda_k} \times 100\%, \tag{10}$$

where $\sum_{i=1}^m \lambda_i = m$ ($i = 1, 2, \dots, m$).

Eigenvalue λ_k ($k = 1 \sim m$), eigenvector matrix $X(m \times n)$, and the time coefficient matrix can be computed using Equations (7)–(9) consecutively. We computed all the main components using the correlation coefficient between the time coefficient matrix and the factor variables.

The meteorological and hydrological observatory is in the countryside in DPR Korea (see Figures 3–5 for the spatial distribution of average annual precipitation and average annual temperature evaluated over the 1961–2010 period, respectively, by interpolation).



Figure 3. Network of meteorological stations (the northern area in DPR Korea).

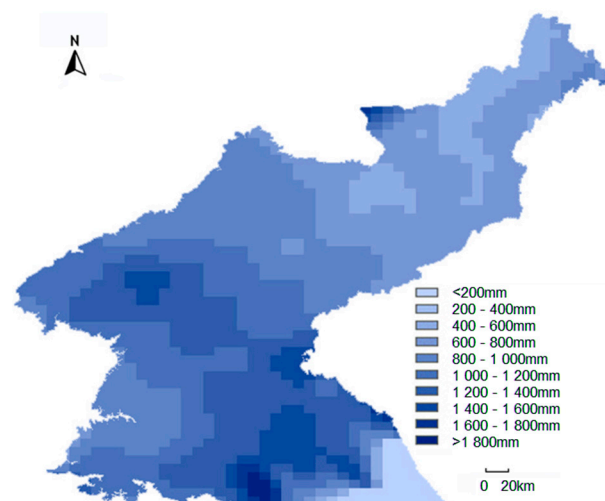


Figure 4. Spatial distribution of average annual precipitation evaluated over the 1961–2010 period (cell size: 10.0 km × 7.1 km).

Table 2 shows the contribution rate and the cumulative contribution rate for the components of factors affecting runoff, calculated using the hydrological observation station data in DPR Korea. The principal component analysis mainly highlights the first four factors. It is obvious that runoff depth in the mentioned regions in Table 2 can be computed using two factors, but for other river basins, at least four factors should be used. Next, the correlation coefficients between time coefficient s and major factors were computed.

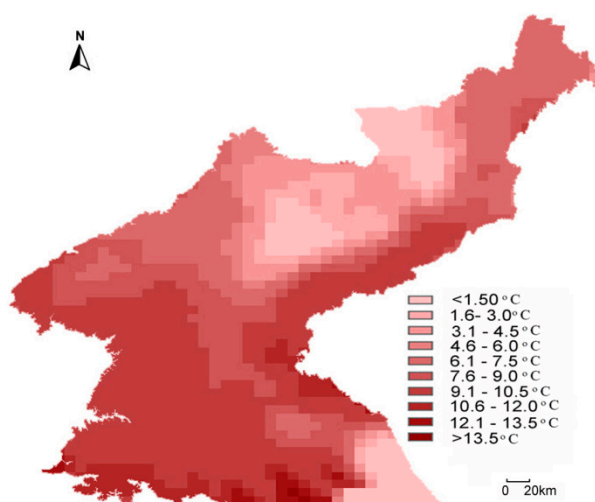


Figure 5. Spatial distribution of average annual temperature evaluated over the 1961–2010 period (cell size: 10.0 km × 7.1 km).

Table 2. The contribution rates for components (%).

No	Region	First Component	Second Component	Third Component	Fourth Component			
			<i>Cumulative</i>	<i>Cumulative</i>	<i>Cumulative</i>			
1	Taedong River Basin	86.6	5.9	92.5	4.1	96.6	1.2	97.8
2	Chongchon River Basin	87.9	6.0	93.9	2.2	96.1	1.8	97.9
3	Ryesong River Basin, Rimjin River Basin	88.1	5.2	93.3	4.8	98.1	1.0	99.1
4	Abrok River Basin	74.9	7.2	82.1	6.4	88.5	3.8	92.3
5	East coast area	66.5	11.1	77.6	8.3	85.9	4.6	89.9
6	Whole DPR Korea	68.5	7.0	75.5	5.2	80.7	4.5	85.2

2.3.1. The Primary Factor: Average Annual Precipitation

Precipitation is obviously the major factor affecting runoff formation. The relationship between precipitation and time coefficient for the first component is computed. Variation in annual precipitation P is considered to be the first factor, and the time coefficient T_1 of the first principal component in the Taedong River Basin is shown in Figures 6 and 7. It is obvious from Figure 6 that the Taedong River Basin has a high correlation of 0.94 between $P(t)$ and $T_1(t)$, while for other river basins, it is 0.78 or more.

It is clear from Table 2 that in the whole area of DPR Korea, the first and second component contribute 68.5% and 7% to the river basin, respectively. It is difficult to identify and directly calculate the second, third, and fourth component. Therefore, they are computed using correlation and regression analysis.

In correlation analysis, the water balance equation is as follows:

$$\left. \begin{aligned} h &= P - z = P - E - u \\ z &= E + u = P - h \\ H &= h + u = P - E \end{aligned} \right\} \quad (11)$$

where h is the runoff depth of surface water; z is loss of precipitation; u is underground runoff depth; and H is whole runoff depth, including surface water and underground water.

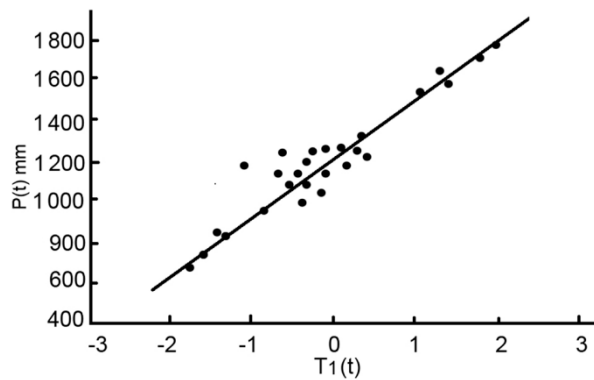


Figure 6. The relationship between $P(t)$ and $T_1(t)$ in the Taedong River Basin.

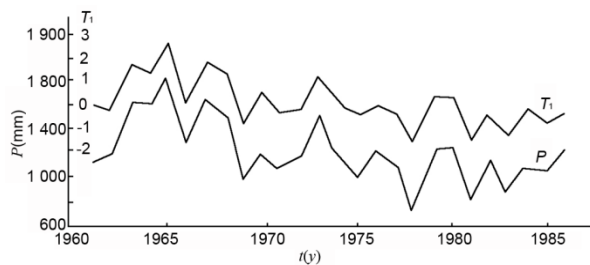


Figure 7. The change curves of $P(t)$ and $T_1(t)$ in the Taedong River Basin.

2.3.2. The Relationship between Average Annual Losses and Average Annual Air Temperature

The second factor can be computed indirectly using a water balance equation, considering annual loss as the effect of precipitation (the first factor) removed up to some level. Generally, most of the annual precipitation is lost by evaporation. Seepage losses are usually ignored while using the water balance relationship for the computation of average annual runoff.

As shown in Figure 8, high correlation exists between average annual precipitation losses z and average annual temperature T in Taedong River. The high correlation coefficient of 0.64 between z and T also denotes that groundwater movement is relatively active in the Taedong River Basin. It is worth noting that there is no linear relationship between z and T , as shown by the lower bound line (dotted line) of distributed dots. The average annual temperature is the primary factor, while the air temperature is the secondary factor affecting evaporation losses.

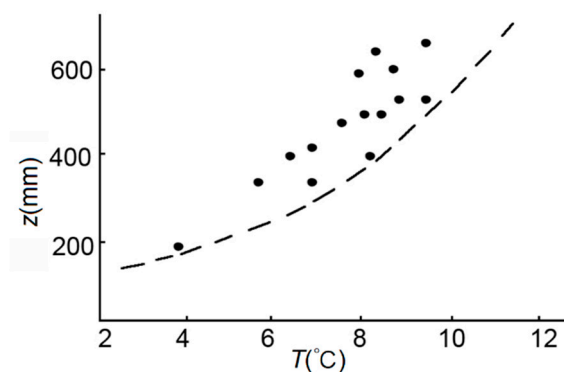


Figure 8. The relationship between the average annual losses z and the average annual temperature T (Taedong River).

2.3.3. The Relationship between Average Annual Losses and Average Annual Precipitation Intensity

Compute evaporation losses by primary and secondary factors affecting evaporation losses and then find out the residue for average annual loss as shown below:

$$\Delta z_1 = z - z' = z - f(P, T) \tag{12}$$

where z' is the calculated evaporation loss.

The residue Δz_1 is high in some areas (northern inland and northern area of the east coast of DPR Korea), as the remaining factors affecting evaporation losses were not considered.

Annual precipitation intensity is defined as:

$$I = \frac{P}{N_p} \tag{13}$$

The residual coefficient is defined as:

$$\eta_{\Delta z_1} = \frac{\Delta z_1}{P} \tag{14}$$

where N_p is the number of annual precipitation days.

The correlation coefficient between I and $\eta_{\Delta z_1}$ is -0.51 , which denotes their inverse relationship (Figure 9). It was stated earlier that evaporation loss has a nonlinear relationship with precipitation intensity, which shows that the number of annual precipitation days (annual precipitation intensity) is one of the major factors affecting the annual runoff formation.

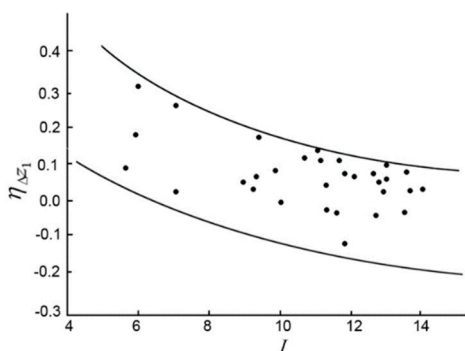


Figure 9. The relation between I and $\eta_{\Delta z_1}$ in DPR Korea.

2.3.4. The Relationship between Continuous Residue and Air Temperature of the Hot Season

Continuous residue (Δz_2) and its coefficient for annual losses can be written as follows:

$$\Delta z_2 = z - f(P, T, I) \tag{15}$$

$$\eta_{\Delta z_2} = \frac{\Delta z_2}{P} \tag{16}$$

It is obvious from the computation that the average range of variation in $\eta_{\Delta z_2}$ is less, compared to $\eta_{\Delta z_1}$, but some new factors affecting $\eta_{\Delta z_2}$ have a large value which cannot be ignored. The evaporation rate is higher in summer compared to winter owing to air temperature. Therefore, the average annual and air temperature of the summer should be considered. The difference in air temperature is given as follows:

$$\Delta t = T' - T \tag{17}$$

where T' is average air temperature from May to October and T is the average annual air temperature.

The relationship between the difference in air temperature (Δt) and the continuous residue coefficient ($\eta_{\Delta z_2}$) is shown in Figure 10. The correlation coefficient between Δt and $\eta_{\Delta z_2}$ is 0.74.

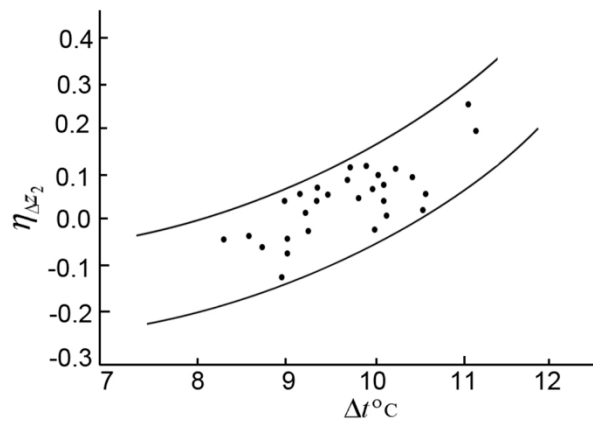


Figure 10. The relationship between Δt and $\eta_{\Delta z_2}$ in DPR Korea.

The air temperature of the hot season (or the difference of air temperature) is one of the main factors affecting annual runoff [4,45]. The difference (or range of variation) between the upper boundary and the lower boundary indicated by a broken line in Figures 9 and 10 is as follows:

$$\eta_{\Delta z_1}(I) = [\eta_{\Delta z_1}(I)]_{up} - [\eta_{\Delta z_1}(I)]_{down} \approx 0.30$$

$$\eta_{\Delta z_2}(\Delta t) = [\eta_{\Delta z_2}(\Delta t)]_{up} - [\eta_{\Delta z_2}(\Delta t)]_{down} \approx 0.20$$

The functional relationship of $\eta_{\Delta z_1}(I)$ and $\eta_{\Delta z_2}(\Delta t)$ is illuminated, as it causes 30% and 20% of the annual precipitation, which leads to the error reduction in annual runoff and/or annual losses computation. It is worth noting that the number of annual precipitation days, the air temperature of the hot season, average annual air temperature, and annual precipitation are the main factors in runoff formation. This can be expressed by the general function, which is given below:

$$h = f(P, T, I, \Delta t) \tag{18}$$

3. Development of an Empirical Average Annual Runoff Model

3.1. Model Development and Description

The general formula can be obtained from the water balance equation and runoff formation factors stated above:

$$\left. \begin{aligned} E &= f(P, T, I, \Delta t) \\ z &= f(P, T, I, \Delta t, \alpha) \end{aligned} \right\} \tag{19}$$

Therefore:

$$\left. \begin{aligned} H &= P - E = f(P, T, I, \Delta t) \\ h &= P - z = f(P, T, I, \Delta t, \alpha) \end{aligned} \right\} \tag{20}$$

where α is a set of variables affecting the underground runoff.

Whole runoff coefficient φ_H and surface runoff coefficient φ_h can be written as follows:

$$\left. \begin{aligned} \varphi_H &= 1 - \eta_E = f(P, T, I, \Delta t) \\ \varphi_h &= 1 - \eta_z = f(P, T, I, \Delta t, \alpha) \end{aligned} \right\} \tag{21}$$

$E \leq z$ and $\eta_E \leq \eta_z$ because most of the losses (z) are caused by evaporation (E). Only E or η_E can be computed by the mathematical method using the observational data and the factors (P , T , and Δt) studied above.

Let us consider the relationship between the loss coefficient η_z , precipitation p , and air temperature t . Draw a curve for the west area of the river basin. The relationship is given as follows:

$$\eta_{Etp} = k_p \eta_{Et} \tag{22}$$

where:

$$k_p = \begin{cases} \left(\frac{P}{1000}\right)^{-1.16} & (P > 1000 \text{ mm}) \\ \left(\frac{P}{1000}\right)^{-0.72} & (P \leq 1000 \text{ mm}) \end{cases} \tag{23}$$

$$\eta_{Et} = \begin{cases} 0.218e^{0.109T} & (T > 11^\circ \text{C}) \\ 0.072e^{0.210t} & (11^\circ \text{C} \geq T > 4^\circ \text{C}) \\ 0.110e^{0.104t} & (T \leq 4^\circ \text{C}) \end{cases} \tag{24}$$

where η_{Etp} is the evaporation loss coefficient defined by the precipitation and air temperature, and k_p is the influence coefficient of annual precipitation.

As shown in Figure 11, some dots are remarkably deflected from the curve drawn by Equation (22). Quantities are computed to characterize the deflected degree for each region, which is given below:

$$\eta_{\Delta z} = \eta_z - \eta_{Etp} \tag{25}$$

$$k'_I = \frac{\eta_z}{\eta_{Etp}} \tag{26}$$

where $\eta_{\Delta z_1}$ is the first residual coefficient of losses, and k'_I is the proportionality coefficient which characterizes the deflected degree between η_z and η_{Etp} .

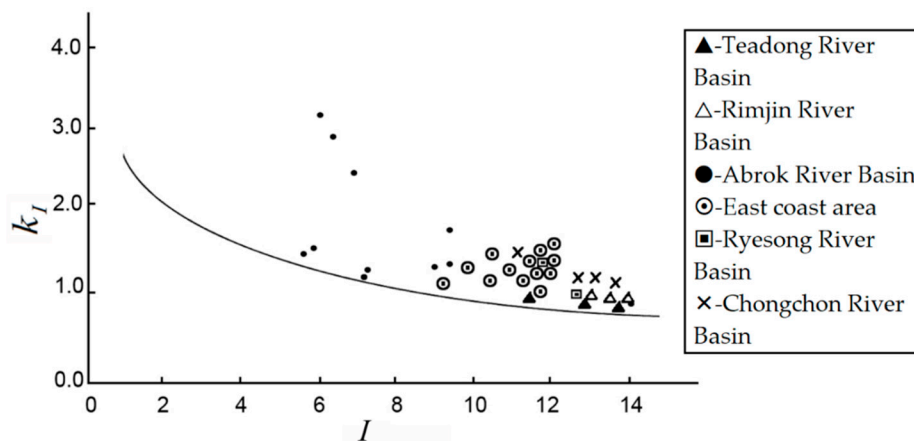


Figure 11. Scatter plot of k'_I vs. I and the relationship curve of $k_I = f(I)$.

The factor defining the first residue Δz_1 and the coefficient $\eta_{\Delta z_1}$ of annual precipitation intensity I have already been investigated. The relationship between k'_I and I is shown in Figure 11, where the $k_I = f(I)$ curve is drawn for the lower boundary condition, which estimates the underground runoff component in the future. Then, the equation of the relationship curve is given below:

$$k_I = 2.98I^{-0.39} \tag{27}$$

where k_I is the influence coefficient of annual precipitation intensity.

The deflection degree of dots from the curve can be computed as follows:

$$\eta_{EtpI} = k_I \eta_{Etp} \tag{28}$$

$$\eta_{\Delta zI} = \eta_z - \eta_{EtpI} \tag{29}$$

$$k'_{\Delta t} = \frac{\eta_z}{\eta_{EtpI}} \tag{30}$$

where η_{EtpI} is the evaporation coefficient calculated by the air temperature, precipitation, and number of annual precipitation days.

Continuous residue Δz_2 or coefficient $\eta_{\Delta z_2}$ is related to the difference between the average temperature T' of the hot season (May to October) and the average annual temperature T . Therefore, the relationship between coefficient $k'_{\Delta t}$ and Δt is analyzed as shown in Figure 12.

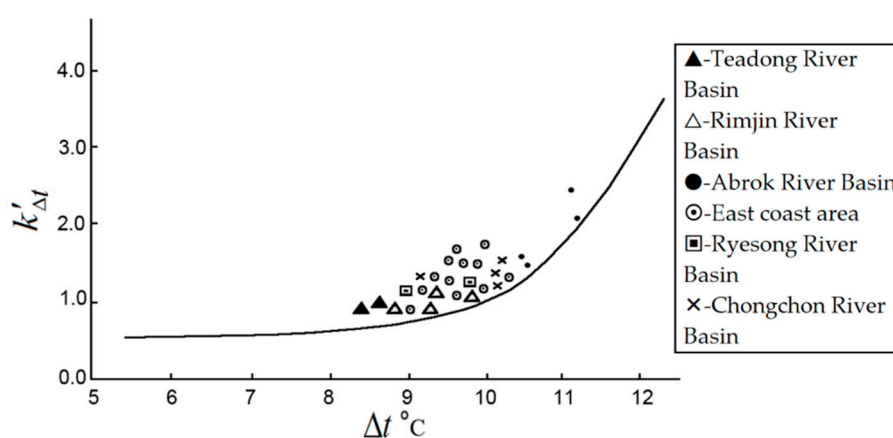


Figure 12. Scatter plot of $k'_{\Delta t}$ vs. Δt and the relationship curve of $k_{\Delta t} = f(\Delta t)$.

The lower bound line of the relationship defines the lost quantity due to the influence of factors ($P, T, I, \Delta t$), as mentioned earlier.

The equation of the relationship curve can be written as follows:

$$k_{\Delta t} = \begin{cases} 0.089e^{0.250\Delta t} (\Delta t > 10 \text{ } ^\circ\text{C}) \\ 0.1973e^{0.1694\Delta t} (\Delta t \leq 10 \text{ } ^\circ\text{C}) \end{cases} \tag{31}$$

The evaporation loss coefficient defined by P, T, I , and Δt can be represented as follows:

$$\eta_{EtpI\Delta t} = \eta_{Et} k_p k_I k_{\Delta t} \tag{32}$$

The third residue Δz_3 and coefficient $\eta_{\Delta z_3}$ can be calculated as follows:

$$\eta_{\Delta z_3} = \eta_z - \eta_{EtpI\Delta t} \tag{33}$$

$$\Delta z_3 = z - P \eta_{EtpI\Delta t} \tag{34}$$

It is worth noting that the values of Δz_3 and $\eta_{\Delta z_3}$ were found to be very small or close to zero except for some special regions. There was a small difference in the computed values for some regions (west coast zone, northern inland, and east coast zone), while a big difference for other regions (Teadong River Basin). It is reasonable to consider Δz_3 as the loss constituent by the underground runoff rather

than evaporation loss by the climate factors. If Δz_3 is the loss component of the underground runoff, then the evaporation coefficient η_E and the evaporation can be represented as follows:

$$\eta_E = \eta_{Et} P I \Delta t = \eta_{Et} k_p k_I k_{\Delta t} \quad (35)$$

$$E = P \eta_{Et} k_p k_I k_{\Delta t} \quad (36)$$

Whole runoff coefficient φ_H and whole runoff depth can be represented as follows:

$$\varphi_H = 1 - \eta_{Et} k_p k_I k_{\Delta t} \quad (37)$$

$$H = P(1 - \eta_{Et} k_p k_I k_{\Delta t}) \quad (38)$$

Equations (37) and (38) are just the average annual runoff models.

This model has high accuracy as well as logical validity, universality, and objectivity that can be applied to all river basins in DPR Korea. Underground runoff can be computed from surface runoff using this model.

The average annual runoff model has some characteristics as follows. The first model considers all the influencing factors of average annual runoff formation and computes them. This model is based on factor analysis, which takes into account annual average precipitation P , air temperature t , annual precipitation intensity I , and hot season temperature t_0 . This model is consistent and has logical validity.

This model is consistent with the physical nature of the natural phenomenon. If $P \rightarrow \infty$, then $k_p \rightarrow 0$, and finally $\eta_E \rightarrow 0$ and $\varphi \rightarrow 1$. Moreover, when precipitation is reduced to zero, i.e., $P \rightarrow 0$, precipitation P_a , called a lower limit precipitation as greater than zero at the moment that runoff reaches to zero, i.e., $Y = 0$ and/or $\phi = 0$, is present, i.e., $P_a > 0$, and P_a is determined by temperature T , precipitation intensity I , and temperature difference Δt .

This model demonstrates that when $P = 0$, not only $\eta_E = 1$ or $\varphi = 0$, but also $\eta_E = 1$ or $\varphi = 0$ subjected to $P = P_a > 0$ according to the values of T , I , and Δt . This model also considers the regional distribution characteristics of influencing factors. The annual runoff map of each factor influencing the annual runoff formation should be developed by a spatial interpolation tool before developing the annual runoff map. All those factors influencing the average annual runoff formation are computed through the Kriging interpolation method [46] (see Figures 4 and 5).

The interpolation accuracy of factor fields was high at a grid cell size 10×10 km, keeping in mind the density of the meteorological observation network in DPR Korea. The model using values of grid cell type is treated linearly values on the same grid cell. Therefore, grid cell size greatly affects the calculation accuracy of models.

This study, to correctly determine grid cell size, analyzed the spatial change of climatic factors according to the distance between observation stations for 200 stations, and the analysis results showed that values of all climatic factors linearly changed within 10~20 km. Additionally, we estimated the interpolation error by calculating values and observed values for grid cell sizes of 10 km, 15 km, and 20 km, respectively. The results as an example of average annual precipitation and average annual air temperature show that their relative errors are within 7~18% in a flat area and mountains for the case of more than 10 km, and within 0.2% for the case of 10 km. The study used a grid cell size of 10 km based on the above research.

Water resources can be exactly evaluated using the average annual runoff model based on the regional distribution of factors affecting the annual runoff formation. Therefore, an annual runoff map of grid cell type can be developed using this model.

3.2. Model Verification on Gauged Area

The proposed average annual runoff model was verified by relative errors between computed values and observed values of runoff depth in 93 gauged sites in DPR Korea. Table 3 shows the number

of sites where the relative error is less than 5%; among the 93 sites, this applies to 83, meaning 89.25% of all sites, and all sites have a relative error of less than 10%. This denotes the usability of the empirical model in the whole area of DPR Korea.

Table 3. Relative errors of calculated runoff depth.

Statistics	Relative Error (%)		
	≤3.0	3.1~5.0	5.1~10.0
The number of sites	62	21	10
Rate occupied sites (%)	66.67	22.58	10.75
Accumulated number of sites	62	83	93
Accumulated rate of sites (%)	66.67	89.25	100

3.3. Cartography of Average Annual Runoff Map

Initially, 200 observation station data were interpolated from 1961 to 2010 using the Kriging interpolation technique for the factors (precipitation P , temperature, T , precipitation intensity I , and temperature difference Δt) affecting annual runoff formation using ArcGIS 9.2 (see Figures 4 and 5). Average annual runoff depth and average annual runoff modulus for the node points of the grid cells was computed using the average annual runoff model. Then, the values of the grid cell center were computed. Using Equation (38), the value of average annual runoff depth in each node points is computed as follows:

$$y_{i,i} = P_{i,j} \left(1 - \eta_{Et(i,j)} \times k_{p(i,j)} \times k_{I(i,j)} \times k_{\Delta t(i,j)} \right) \quad (39)$$

where:

$\eta_{Et(i,j)}$ is the influence coefficients of average annual temperature in grid cell i, j ;

$k_{p(i,j)}$ is average annual precipitation in grid cell i, j ;

$k_{I(i,j)}$ is average annual precipitation intensity in grid cell i, j ;

$k_{\Delta t(i,j)}$ is the temperature of hot season affecting the annual evaporation in grid cell i, j .

A value of any grid cell center point is computed as the mean value of its four nodal points (Equation (40)).

$$Y_{i,j} = (y_a + y_b + y_c + y_d) / 4 \quad (40)$$

The central values were updated, which leads to the completion of the average annual runoff map.

Water resources information can be easily obtained from the ungauged region using the runoff map developed by GIS spatial analysis tools. Average annual runoff depth can be computed in the upper basin of any river cross section using ArcGIS 9.2 and the runoff map of grid cell type using the weighted average method as follows:

$$Y = \frac{1}{n} \sum_i \sum_j Y_{ij} k_{ij} \quad (41)$$

where Y_{ij} is average annual runoff depth in a grid cell i, j ; n is the number of grid cells included in the selected area; and k_{ij} is the area weight in grid cell i, j , namely:

$$k_{ij} = \frac{\Delta f_{ij}}{\Delta F} \quad (42)$$

where ΔF is the area of a grid cell having the size of $10 \text{ km} \times 10 \text{ km}$, i.e., $\Delta F = 100 \text{ km}^2$; and Δf_{ij} (km^2) is the component area occupied on the grid cell.

$k_{ij} = 1.0$ and $k_{ij} \leq 1.0$ for completely and partially contained grid cells within the watershed boundary, respectively. Average annual runoff depth can be obtained directly from the average annual

runoff map on the river basin, where the basin area is smaller than 100~200 km², i.e., $F \leq 100 \sim 200 \text{ km}^2$. The abovementioned procedure is automatically executed by a spatial analysis tool in GIS.

4. Application on Tumen River Basin

4.1. The Natural Geographic Characteristics of Tumen River Basin

Tumen River is a boundary river passing through the border of DPR Korea, China, and Russia (see Figure 13). The area and length of the Tumen River Basin is 32,920.0 km² and 547.8 km, respectively. Tumen River is the second longest, and the basin area is the third largest in DPR Korea. The average annual precipitation of the river basin is below 600 mm. It is smaller than other basins because of the influence of the Hamgyong Mountain Range. Figures 14 and 15 show the map of average annual precipitation and the map of average annual temperature evaluated for 50 years in the Tumen River Basin.



Figure 13. Tumen River Basin (DPR Korea side).

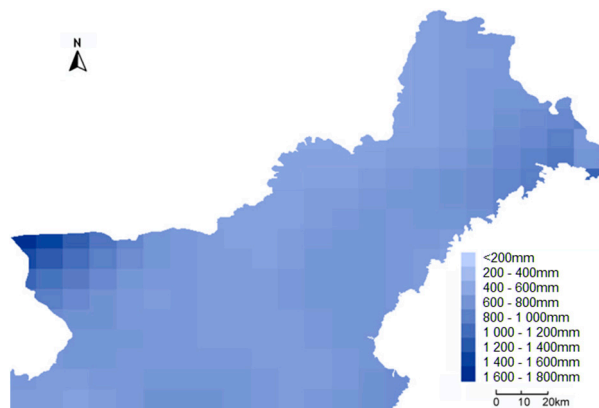


Figure 14. The map of average annual precipitation evaluated for 50 years in the Tumen River Basin (DPR Korea side).

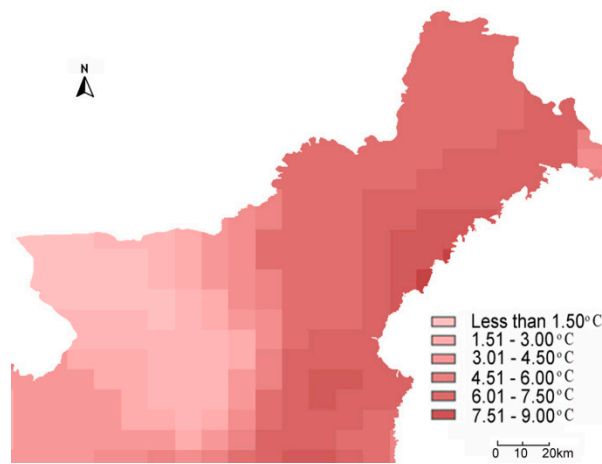


Figure 15. The map of average annual temperature evaluated for 50 years in the Tumen River Basin (DPR Korea side).

4.2. Water Resources of Tumen River Basin (DPR Korea Side)

The proposed average annual runoff model was applied to the Tumen River Basin (DPR Korea side) for water resources computation. Figures 16 and 17 show the map of average annual evaporation and average annual runoff depth of the Tumen River Basin (DPR Korea side), respectively. The mean value of average annual precipitation, average annual evaporation, average annual runoff depth, average annual runoff, and total water resources of the Tumen River Basin are approximately 604 mm, 254 mm, 350 mm, $11 \ell/s \cdot km^2$, and $3,707,829 \times 10^3 m^3$, respectively. It is evident from the results that great care is needed to protect water resources for ecological environment protection, establishment and implementation of the strategy for supports development because the water resources of the Tumen River Basin are running short due to exceeding evaporation, which is comparatively greater than in other river basins.

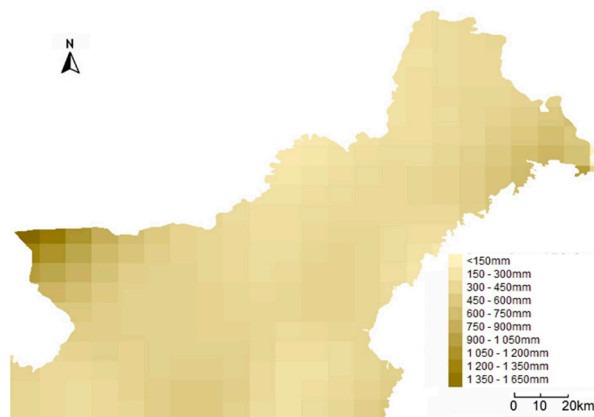


Figure 16. The map of average annual evaporation evaluated for 50 years in the Tumen River Basin (DPR Korea side).

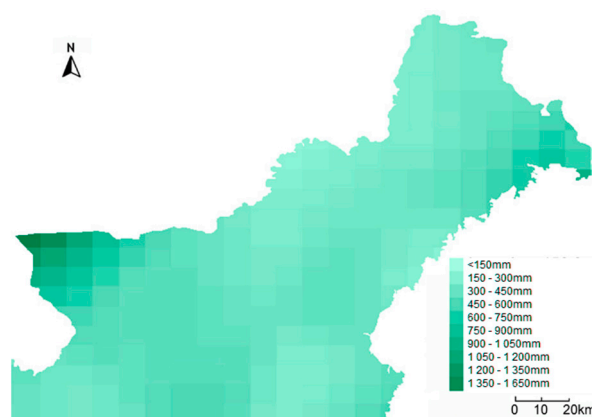


Figure 17. The map of average annual runoff depth evaluated for 50 years in the Tumen River Basin (DPR Korea side).

5. Discussion

At present, it seems we are more interested in modeling runoff at finer resolutions, i.e., daily and subdaily scales, rather than an annual scale. However, such a straightforward empirical model is also a useful management tool. An average annual runoff model was applied to assess the water resources of the river basin and can be used to determine average annual runoff in ungauged basins. This method is widely used for the development and management of water resources by the water-related institutes and the design agencies in DPR Korea.

Water resources can be easily computed in any region by a spatial analysis tool of GIS. The study of the distributed hydrologic model considering the physical, geographical, and meteorological factors influencing the runoff formation is one of the current trends in hydrological studies. Spatial variation in all those factors affecting runoff formation can be easily obtained by emerging technology such as 3S (GIS, RS, GPS). The distributed parameter model is more efficient than the lumped parameter model. This model develops a water resources map for the whole country in a very short time compared to the traditional models. The accuracy of the distributed model partly depends on the interpolation accuracy of the influencing factors in the model. In this study, variation in meteorological factors by topography was not considered. Due to a long length of 50 years of records in the case study of the Tumen River Basin, climate change may be taken into consideration in future work, and this is an important topic on recent water resource management studies [15,18,47–49]. The proposed statistical model can also be used for evaluation of climate change and human activity influence on the water resources of DPR Korea.

The formation of surface runoff–infiltration and Hortonian overland flow [36,50] is disregarded in the modeling process since the spatial–temporal scale in this study is much larger. The in situ process of runoff formation was not described in the model. It may be an interesting topic to be considered in future studies that focus on how to combine the infiltration and Hortonian flow process in our empirical model to improve the model accuracy.

DPR Korea is characterized by a combination of a continental climate and an oceanic climate. The calibrated model in the work can rationally be used on other countries or regions where runoff formation condition is the same as DPR Korea, and the proposed approach has universal applicability, since it is deduced from the basic water balance model. To apply to other countries or regions, it needs to consider different climate, runoff formation condition, and data availability in the local area, and the empirical relationship may differ. Hydrological models should be derived considering the meteorological, natural geographical conditions, and hydrological characteristics of the study area.

Comparison with more complex distributed hydrological models [51] like SWAT is able to support the verification of this new statistical model. However, due to data limitation, this is an issue at this stage.

6. Conclusions

This work developed an empirical hydrological model to provide fundamental information on the principal components of the water balance period in a predefined area over a selected time. It can also be used for future projections to some extent. PCA identified the four major factors contributing to the variation of average annual runoff in DPR Korea. The proposed average annual runoff model was composed of average annual precipitation, average precipitation intensity, average annual air temperature, and hot seasonal air temperature. It was proven through hydrologic data for 93 river basins of DPR Korea that the proposed statistical model can sufficiently reflect the physical nature of runoff formation in DPR Korea. Kriging interpolation tools of Arc GIS 9.2 were used to estimate the spatial distribution of factors affecting average annual runoff formation. A 10 km × 10 km grid cell size was used to interpolate factor fields, which was determined through analysis for spatial change of climate elements in 200 weather stations of DPR Korea. Average annual runoff depth for each grid cell can be easily computed through Equation (39) using the spatially distributed fields of factors affecting annual runoff formation. Further, in this study, a grid cell type runoff map was developed by the average annual runoff data of each grid cell and the proposed cartography of the average annual runoff map and use method. The case study on the Tumen River Basin demonstrates that this research work is highly significant for decision makers as it highlights variations in water resources, which are important for water resources development and management. The statistical–distributed hydrological model facilitates hydrologists in water resources assessment and information sharing in an ungauged area.

Author Contributions: T.R., conceptualization, data collection, formal analysis, software development, and writing original draft; J.J., conceptualization, writing original draft, review and editing the manuscript, supervision, methodology, and funding acquisition; S.B., imputing ideas, condensing the presentation of findings, and reviewing and editing the manuscript; T.P., reviewing and editing the manuscript and visualization.

Funding: This research was funded by the National Natural Science Foundation of China (Grant No. 51509061), the open research fund of State Key Laboratory of Urban Water Resource and Water Environment (MH20180645). Additional support was provided by the Southern University of Science and Technology (Grant No. G01296001).

Acknowledgments: We acknowledge the support of the National Natural Science Foundation of China and International Office in Harbin Institute of Technology to make this research possible. We wish to thank Afed Khan for language correction. We thank the anonymous reviewers for their thorough and thoughtful comments, which helped to improve this manuscript.

Conflicts of Interest: The authors declare no conflict of interest.

References

1. Kannan, N.; Santhi, C.; Arnold, J.G. Development of an automated procedure for estimation of the spatial variation of runoff in large river basins. *J. Hydrol.* **2008**, *359*, 1–15. [[CrossRef](#)]
2. Wang, Y.; Lei, X.; Liao, W.; Jiang, Y.; Huang, X.; Liu, J.; Song, X.; Wang, H. Monthly spatial distributed water resources assessment: A case study. *Comput. Geosci.* **2012**, *45*, 319–330. [[CrossRef](#)]
3. Xu, C.-Y.; Singh, V.P. Review on Regional Water Resources Assessment Models under Stationary and Changing Climate. *Water Res. Manag.* **2004**, *18*, 591–612. [[CrossRef](#)]
4. Hickel, K.; Zhang, L. Estimating the impact of rainfall seasonality on mean annual water balance using a top-down approach. *J. Hydrol.* **2006**, *331*, 409–424. [[CrossRef](#)]
5. Church, M.R.; Bishop, G.D.; Cassell, D.L. Maps of regional evapotranspiration and runoff/precipitation ratios in the northeast United States. *J. Hydrol.* **1995**, *168*, 283–298. [[CrossRef](#)]
6. Bishop, G.D.; Church, M.R. Automated approaches for regional runoff mapping in the northeastern United States. *J. Hydrol.* **1992**, *138*, 361–383. [[CrossRef](#)]
7. Bishop, G.D.; Church, M.R. Mapping long-term regional runoff in the eastern United States using automated approaches. *J. Hydrol.* **1995**, *169*, 189–207. [[CrossRef](#)]
8. Hickel, K.; Zhang, L. The Impact of Rainfall Seasonality on Mean Annual Water Balance in Catchments with Different Land Cover. In *CRC for Catchment Hydrology*; eWater: Canberra, Australia, 2003.

9. Milly, P.C.D. Climate, interseasonal storage of soil water, and the annual water balance. *Adv. Water Res.* **1994**, *17*, 19–24. [[CrossRef](#)]
10. Arnell, N.W. Grid mapping of river discharge. *J. Hydrol.* **1995**, *167*, 39–56. [[CrossRef](#)]
11. Menció, A.; Folch, A.; Mas-Pla, J. Identifying key parameters to differentiate groundwater flow systems using multifactorial analysis. *J. Hydrol.* **2012**, *472–473*, 301–313. [[CrossRef](#)]
12. Singh, R.; Archfield, S.A.; Wagener, T. Identifying dominant controls on hydrologic parameter transfer from gauged to ungauged catchments—A comparative hydrology approach. *J. Hydrol.* **2014**, *517*, 985–996. [[CrossRef](#)]
13. Christine, L.G.; John, D.A.; Scott, V.O. Mapping monthly precipitation, temperature, and solar radiation for Ireland with polynomial regression and a digital elevation model. *Clim. Res.* **1998**, *10*, 35–49.
14. Milly, P.C.D.; Eagleson, P.S. Effects of spatial variability on annual average water balance. *Water Resour. Res.* **1987**, *23*, 2135–2143. [[CrossRef](#)]
15. Daly, C.; Neilson, R.P.; Phillips, D.L. A Statistical-Topographic Model for Mapping Climatological Precipitation over Mountainous Terrain. *J. Appl. Meteorol.* **1994**, *33*, 140–158. [[CrossRef](#)]
16. McCabe, G.J.; Wolock, D.M. Temporal and spatial variability of the global water balance. *Clim. Chang.* **2013**, *120*, 375–387. [[CrossRef](#)]
17. Boughton, W.; Chiew, F. Estimating runoff in ungauged catchments from rainfall, PET and the AWBM model. *Environ. Model. Softw.* **2007**, *22*, 476–487. [[CrossRef](#)]
18. Arora, V.K. The use of the aridity index to assess climate change effect on annual runoff. *J. Hydrol.* **2002**, *265*, 164–177. [[CrossRef](#)]
19. Helfer, F.; Lemckert, C.; Zhang, H. Impacts of climate change on temperature and evaporation from a large reservoir in Australia. *J. Hydrol.* **2012**, *475*, 365–378. [[CrossRef](#)]
20. Krug, W.R.; Gebert, W.A.; Graczyk, D.J.; Stevens, D.L., Jr.; Rochelle, B.P.; Church, M.R. *Map of Mean Annual Runoff for the Northeastern, Southeastern, and Mid-Atlantic United States, Water Years, 1951–1980*; Water-Resources Investigations Report, 88-4094; U.S. Geological Survey: Reston, VA, USA, 1990; p. 15.
21. Zhou, X.; Zhang, Y.; Wang, Y.; Zhang, H.; Vaze, J.; Zhang, L.; Yang, Y.; Zhou, Y. Benchmarking global land surface models against the observed mean annual runoff from 150 large basins. *J. Hydrol.* **2012**, *470–471*, 269–279. [[CrossRef](#)]
22. David, M.W.; Gregory, J.M. Explaining spatial variability in mean annual runoff in the conterminous United States. *Clim. Res.* **1999**, *11*, 149–159.
23. Smith, M.B.; Koren, V.I.; Zhang, Z.; Reed, S.M.; Pan, J.-J.; Moreda, F. Runoff response to spatial variability in precipitation: An analysis of observed data. *J. Hydrol.* **2004**, *298*, 267–286. [[CrossRef](#)]
24. Kirkby, M.J.; Bracken, L.J.; Shannon, J. The influence of rainfall distribution and morphological factors on runoff delivery from dryland catchments in SE Spain. *CATENA* **2005**, *62*, 136–156. [[CrossRef](#)]
25. Ignatov, A.V.; Kichigina, N.V. Modeling elements and geographical factors of formation of the monthly runoff as exemplified by the Kuda river. *Geogr. Nat. Res.* **2010**, *31*, 396–402. [[CrossRef](#)]
26. Greenwood, A.J.B.; Benyon, R.G.; Lane, P.N.J. A method for assessing the hydrological impact of afforestation using regional mean annual data and empirical rainfall–runoff curves. *J. Hydrol.* **2011**, *411*, 49–65. [[CrossRef](#)]
27. Chang, H.; Johnson, G.; Hinkley, T.; Jung, I.-W. Spatial analysis of annual runoff ratios and their variability across the contiguous U.S. *J. Hydrol.* **2014**, *511*, 387–402. [[CrossRef](#)]
28. Westra, S.; Brown, C.; Lall, U.; Sharma, A. Modeling multivariable hydrological series: Principal component analysis or independent component analysis? *Water Resour. Res.* **2007**, *43*. [[CrossRef](#)]
29. Wotling, G.; Bouvier, C.; Danloux, J.; Fritsch, J.M. Regionalization of extreme precipitation distribution using the principal components of the topographical environment. *J. Hydrol.* **2000**, *233*, 86–101. [[CrossRef](#)]
30. Reder, A.; Rianna, G.; Vezzoli, R.; Mercogliano, P. Assessment of possible impacts of climate change on the hydrological regimes of different regions in China. *Adv. Clim. Chang. Res.* **2016**, *7*, 169–184. [[CrossRef](#)]
31. Beven, K.; Robert, E. Horton’s perceptual model of infiltration processes. *Hydrol. Proc.* **2004**, *18*, 3447–3460. [[CrossRef](#)]
32. Dias, L.C.P.; Macedo, M.N.; Costa, M.H.; Coe, M.T.; Neill, C. Effects of land cover change on evapotranspiration and streamflow of small catchments in the Upper Xingu River Basin, Central Brazil. *J. Hydrol. Reg. Stud.* **2015**, *4*, 108–122. [[CrossRef](#)]

33. Yang, P.; Xia, J.; Zhan, C.; Qiao, Y.; Wang, Y. Monitoring the spatio-temporal changes of terrestrial water storage using GRACE data in the Tarim River basin between 2002 and 2015. *Sci. Total Environ.* **2017**, *595*, 218–228. [[CrossRef](#)] [[PubMed](#)]
34. Beven, K.; Binley, A. The future of distributed models: Model calibration and uncertainty prediction. *Hydrol. Proc.* **1992**, *6*, 279–298. [[CrossRef](#)]
35. Beven, K.J. *Rainfall-Runoff Modelling: The Primer*; Wiley: Hoboken, NJ, USA, 2011.
36. Beven, K. Infiltration excess at the Horton Hydrology Laboratory (or not?). *J. Hydrol.* **2004**, *293*, 219–234. [[CrossRef](#)]
37. De Jong van Lier, Q.; Sparovek, G.; Flanagan, D.C.; Bloem, E.M.; Schnug, E. Runoff mapping using WEPP erosion model and GIS tools. *Comput. Geosci.* **2005**, *31*, 1270–1276. [[CrossRef](#)]
38. Milewski, A.; Sultan, M.; Yan, E.; Becker, R.; Abdeldayem, A.; Soliman, F.; Gelil, K.A. A remote sensing solution for estimating runoff and recharge in arid environments. *J. Hydrol.* **2009**, *373*, 1–14. [[CrossRef](#)]
39. Cheng, Q.; Ko, C.; Yuan, Y.; Ge, Y.; Zhang, S. GIS modeling for predicting river runoff volume in ungauged drainages in the Greater Toronto Area, Canada. *Comput. Geosci.* **2006**, *32*, 1108–1119. [[CrossRef](#)]
40. Graczyk, D.J.; Gebert, W.A.; Krug, W.R.; Allord, G.J. *Maps of Runoff in the Northeastern Region and the Southern Blue Ridge Province of the United States During Selected Periods in 1983–1985*; Open-File Report, 87-106; U.S. Geological Survey: Reston, VA, USA, 1987; p. 12.
41. Sauquet, E. Mapping mean annual river discharges: Geostatistical developments for incorporating river network dependencies. *J. Hydrol.* **2006**, *331*, 300–314. [[CrossRef](#)]
42. Yan, Z.; Xia, J.; Gottschalk, L. Mapping runoff based on hydro-stochastic approach for the Huaihe River Basin, China. *J. Geogr. Sci.* **2011**, *21*, 441–457. [[CrossRef](#)]
43. Milly, P.C.D. Climate, soil water storage, and the average annual water balance. *Water Resour. Res.* **1994**, *30*, 2143–2156. [[CrossRef](#)]
44. Li, G.; Zhang, F.; Jing, Y.; Liu, Y.; Sun, G. Response of evapotranspiration to changes in land use and land cover and climate in China during 2001–2013. *Sci. Total Environ.* **2017**, *596–597*, 256–265. [[CrossRef](#)]
45. Caracciolo, D.; Deidda, R.; Viola, F. Analytical estimation of annual runoff distribution in ungauged seasonally dry basins based on a first order Taylor expansion of the Fu's equation. *Water Res.* **2017**, *109*, 320–332. [[CrossRef](#)]
46. Bostan, P.A.; Heuvelink, G.B.M.; Akyurek, S.Z. Comparison of regression and kriging techniques for mapping the average annual precipitation of Turkey. *Int. J. Appl. Earth Obs. Geoinf.* **2012**, *19*, 115–126. [[CrossRef](#)]
47. Li, L.; Zhang, L.; Xia, J.; Gippel, C.J.; Wang, R.; Zeng, S. Implications of Modelled Climate and Land Cover Changes on Runoff in the Middle Route of the South to North Water Transfer Project in China. *Water Res. Manag.* **2015**, *29*, 2563–2579. [[CrossRef](#)]
48. Chang, J.; Zhang, H.; Wang, Y.; Zhu, Y. Assessing the impact of climate variability and human activities on streamflow variation. *Hydrol. Earth Syst. Sci.* **2016**, *20*, 1547–1560. [[CrossRef](#)]
49. Chiew, F.H.S.; Teng, J.; Vaze, J.; Post, D.A.; Perraud, J.M.; Kirono, D.G.C.; Viney, N.R. Estimating climate change impact on runoff across southeast Australia: Method, results, and implications of the modeling method. *Water Resour. Res.* **2009**, *45*. [[CrossRef](#)]
50. Delfs, J.O.; Park, C.H.; Kolditz, O. A sensitivity analysis of Hortonian flow. *Water Res.* **2009**, *32*, 1386–1395. [[CrossRef](#)]
51. Devia, G.K.; Ganasri, B.P.; Dwarakish, G.S. A Review on Hydrological Models. *Aquat. Procedia* **2015**, *4*, 1001–1007. [[CrossRef](#)]

